Oxygen adsorption and ordering on Ru$(10\bar{1}0)$

Alessandro Baraldi* and Silvano Lizzit
Sincrotrone Trieste, Area Science Park, Basovizza 34012 Trieste, Italy

Giovanni Comelli
Dipartimento di Fisica, Universitá di Trieste, 34127 Trieste and Laboratorio TASC-INFM, Area Science Park, Basovizza 34012 Trieste, Italy

Giorgio Paolucci
Sincrotrone Trieste, Area Science Park, Basovizza 34012 Trieste, Italy
(Received 30 August 2000; published 28 February 2001)

The dissociative oxygen chemisorption on the Ru$(10\bar{1}0)$ surface has been studied by monitoring the changes of the O $1s$ and Ru $3d_{5/2}$ core levels and by measuring the evolution of the diffraction pattern during oxygen exposure at 270 K. The sensitivity of core level binding energies to different geometrical configurations, together with the measurements of the oxygen-induced diffraction spot profile along the [0001] and $[1\bar{2}10]$ directions, permit us to follow the details of formation of the $c(2\times4)$ and the $(2\times1)p2mg$ ordered structures.

DOI: 10.1103/PhysRevB.63.115410 PACS number(s): 82.80.Pv, 68.35.Bs, 79.60.Dp, 61.14.Hg

I. INTRODUCTION

Oxygen chemisorption on fcc(110) transition metal surfaces has been a widely studied subject in surface science during the last few decades. This effort is mainly motivated by the importance of oxygen as surface species in many heterogeneously catalyzed reactions. Moreover oxygen adsorption induces on Cu, Ni, Pd, Ag, and Rh a surface reconstruction, in which a considerable mass transport results in formation of missing or added rows. Surprisingly, only few investigations have been performed on the (110) fcc-like termination of Ru, i.e., the $(10\bar{1}0)$ surface, and in particular oxygen adsorption on ruthenium has been studied by Orent *et al.*[1] in the seventies and by Poulston *et al.*[2] Only recently Schwegmann *et al.*[3] presented detailed results of a structural investigation of the Ru$(10\bar{1}0)$ system, where a combination of low energy electron diffraction (LEED), high resolution electron energy loss spectroscopy (HREELS) and density functional theory (DFT) calculations has been applied. On this surface oxygen adsorption leads to the formation of a $c(2\times4)$ and a $(2\times1)p2mg$ ordered structure, at coverage of 0.5 and 1 ML, respectively. In both structures oxygen adsorption is determined to occur at threefold hcp sites, in a zig-zag arrangement along the $[1\bar{2}10]$ direction.

This paper adds spot profile analysis LEED (SPA-LEED) and x-ray photoelectron spectroscopy (XPS) data to the description of the O-Ru$(10\bar{1}0)$ system. Qualitative and quantitative information about the adsorption kinetics, oxygen ordered island formation and occupation of the adsorption sites have been obtained.

II. EXPERIMENT

The experiments were carried out in two different UHV chambers. The synchrotron radiation photoemission experiments were performed at the SuperESCA beamline of ELETTRA.[4] The chamber is equipped with a VSW class 150 16-channels electron energy analyser, LEED and mass spectrometer. The beamline provides photons between 180 and 1000 eV with a maximum resolving power of 10^4. In order to acquire the XPS spectra at a fast rate during the oxygen uptake we used the following experimental conditions: (i) the photon beam was impinging the sample at grazing angle (5°) with the electron energy analyzer at 45° respect to the sample normal, and (ii) the beamline and the analyzer were operated at a photon energy of 630 eV with an overall energy resolution of 400 meV for measuring the O $1s$, while $h\nu = 400$ eV was used in order to measure the Ru $3d_{5/2}$ signal with a resolution of 65 meV.

The second UHV chamber, which is located in the Surface Science Laboratory of Sincrotrone Trieste, is equipped with an Omicron SPA-LEED system which allows the measurement of the diffraction spots line shape. The transfer width of the instrument is better than 700 Å at electron kinetic energy of 115 eV.

The sample was cleaned by cycles of Ar^+ bombardment at 1 keV and 400 K, annealing to 1400 K and oxygen treatment at 1000–1100 K. During the cooling the sample was reduced in hydrogen (1×10^{-7} mbar) in order to remove any residual oxygen. Immediately before oxygen exposure the sample was flashed to 600 K to remove any residual adsorbed hydrogen, water or carbon monoxide. The oxygen adsorption experiments have been done by exposing the clean Rh surface to O_2 at a constant temperature of 270 K.

III. RESULTS

A. Spot profile analysis–low energy electron diffraction

It is known that at room temperature molecular oxygen adsorbs dissociatively on the Ru$(10\bar{1}0)$ surface.[2,3] At this temperature thermal desorption of oxygen can be neglected;

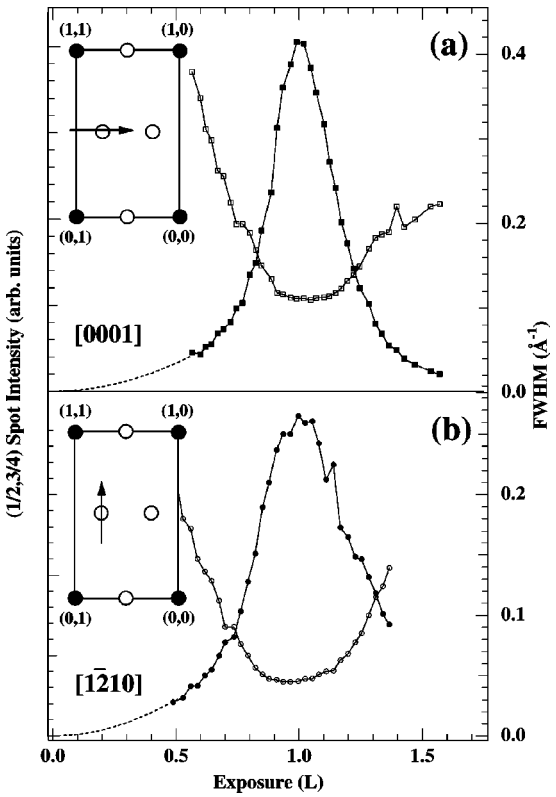

FIG. 1. Intensity (filled markers) and FWHM (open markers) vs dose (Langmuir) of the (1/2,3/4) diffraction spot along the [0001] (a) and [$1\bar{2}10$] direction (b) at $T=270$ K.

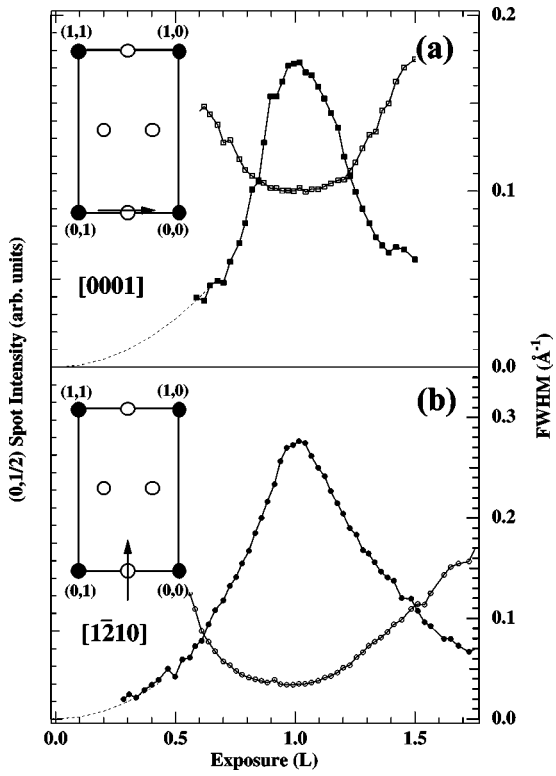

FIG. 2. Intensity (filled markers) and FWHM (open markers) vs dose (Langmuir) of the (0,1/2) diffraction spot along the [0001] (a) and [$1\bar{2}10$] direction (b) at $T=270$ K.

the O atoms are bounded to the surface, but the mobility is sufficiently high to reach thermodynamic two-dimensional equilibrium as manifested by the formation of a sequence of two ordered overlayer phases. The Spot Profile LEED measurements of the oxygen induced half order diffraction beams have been performed at constant temperature. Images and line profile scans of the diffraction beams along the [$1\bar{2}10$] and [0001] crystallographic directions have been taken at $T=270$ K while dosing oxygen at 2×10^{-9} mbar. The temperature of the sample was kept constant to within ±2 K. The SPA-LEED was operated at 82 eV electron-beam energy.

The first distinguishable LEED pattern appears after an exposure of about 0.5 L and is characterized by (1/2,3/4) and (0,1/2) diffraction spots, as shown in Figs. 1 and 2, where the $I_{1/2,3/4}$ and $I_{0,1/2}$ intensities and the widths of the diffraction spots are plotted against exposure. The peak intensity and the full width at half maximum have been obtained by fitting the spot profiles with a convolution of a Lorentzian and a Gaussian function, after background subtraction (obtained by a linear fit of the tails of the peaks). Along the [$1\bar{2}10$] direction [Fig. 1(b)] the spots are quite sharp, while [Fig. 1(a)] broadening along the [0001] direction indicates the development of anisotropic ordering process. With increasing oxygen exposure the spots become sharper and narrower indicating that the structural transformations are governed by formation of long-range ordered islands. At an exposure of about 1.0 L the (1/2,3/4) and (0,1/2) spot reach the maximum intensity and minimum FWHM, indicating the formation of the $c(2\times4)$ structure. Upon increasing the exposure (>1 L) the (1/2,3/4) spots decrease in intensity and coalesce at saturation into the (1/2,1) spot. The $I_{1/2,1}$ curve and the FWHM of the (1/2,1) spot profile measured along the [0001] (a) and the [$1\bar{2}10$] (b) directions are plotted in Fig. 3. This structure is also composed of island about 2 times wider along the [$1\bar{2}10$] direction than along the [0001], as judged by the FWHM of the diffraction spot. At saturation a non-primitive (2×1) structure is reached. For normal incidence, all fractional order spots $(n+1/2,0)$ with $n=0,\ \pm1,\ \pm2,\ldots$, are missing, indicating the existence of a glide line along the [0001] direction, as previously reported by Poulston *et al.*[2] and by Schwegmann *et al.*[3] In order to calibrate the oxygen coverage in the SPA-LEED data, we used the O 1*s* core-level XPS uptakes, assuming that at saturation (20 L) the coverage is 1 ML. With this procedure, as reported in the next section, the coverage of the best $c(2\times4)$ structure results to be 0.51 ± 0.01 ML, in good agreement with the previous studies.[2,3]

By varying the oxygen coverage the (1/2,3/4) spot moves towards the (1/2,1) spot. The spot position in the [0001] direction is shown in Fig. 4 as a function of oxygen exposure. Near saturation there is some ambiguity in the determination of this quantity because the spots are close together and even overlap with the (1/2,1) spot. The spot position varies linearly for coverages Θ below 0.42 ML and above

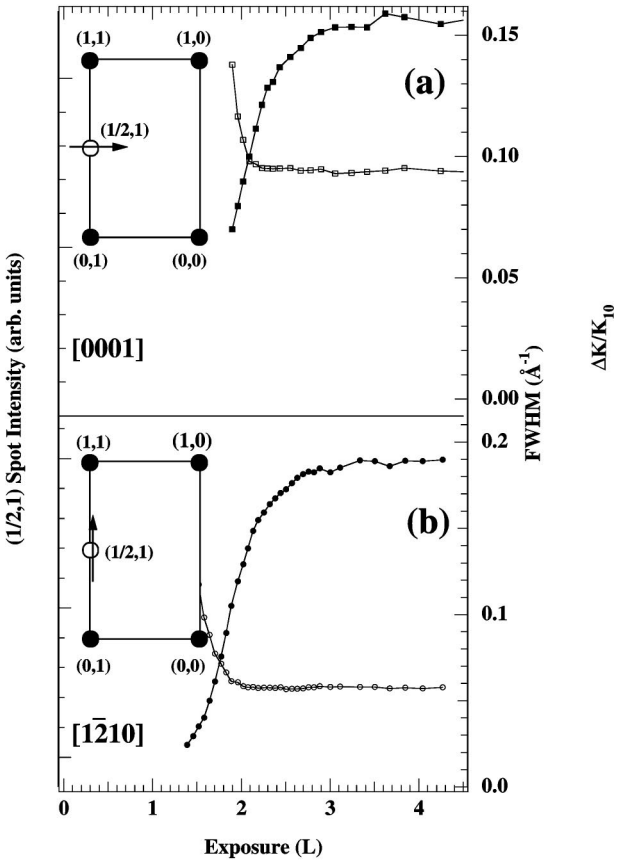

FIG. 3. Intensity (filled markers) and FWHM (open markers) vs oxygen dose (Langmuir) for the (1/2,1) diffraction spot along the [0001] (a) and [1$\bar{2}$10] direction (b) at $T=270$ K.

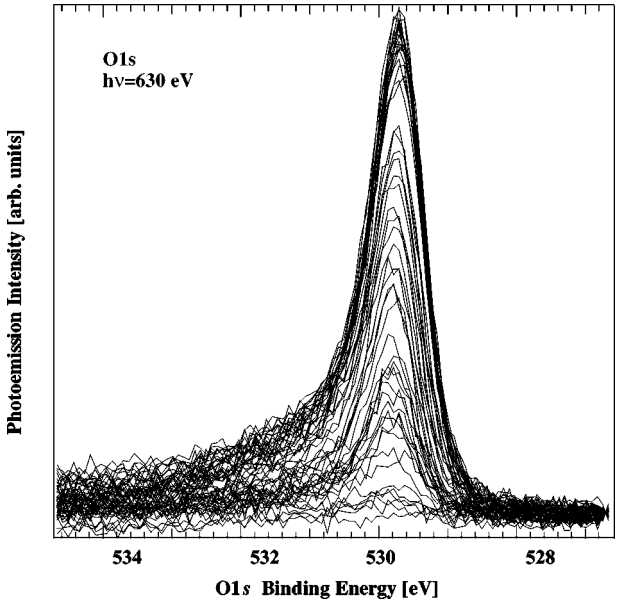

FIG. 5. O 1s core level photoemission spectra measured while oxygen dosing at $T=270$ K and $h\nu=630$ eV.

0.58 ML, while in between stays nearly constant. Upon raising the temperature, the intensities of the $c(2\times4)$ superstructure beams decrease far below of the desorption onset (1050 K), indicating the occurrence of a continuos order-disorder phase transition, as previously observed.[2] The critical temperature T_c was determined to be 350 K by measuring the temperature at which the diffraction spots begin to broaden in both [0001] and [1$\bar{2}$10] crystallographic directions. However, since the spots completely disappear only above 570 K the transition is not very sharp thus indicating that finite size effects could have a strong influence on the transition.[5,6]

B. X-Ray photoelectron spectroscopy

Figure 5 shows a set of O 1s spectra collected during the oxygen uptake at 270 K. The intensity and position of the core level peaks have been quantified by fitting the curves with a Doniach-Sunijc function convoluted with a Gaussian function.[7] The results of the analysis are plotted in Fig. 6. The O 1s binding energy position (open markers) of the peak changes for doses higher than 1 L. At this exposure the

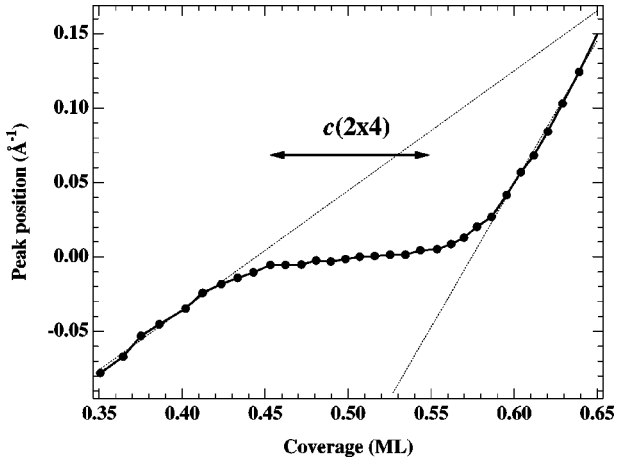

FIG. 4. (1/2,3/4) diffraction spot peak position along the [0001] direction as a function of oxygen coverage.

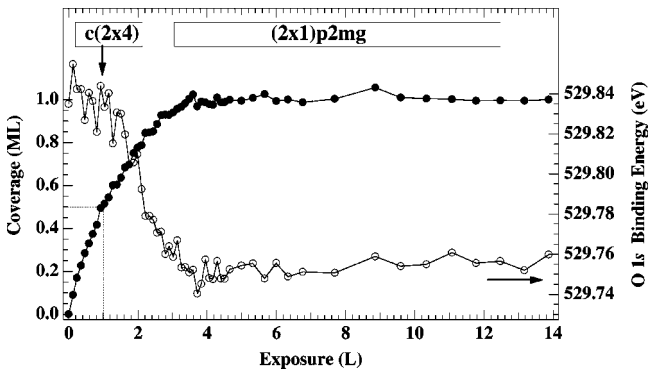

FIG. 6. Oxygen coverage (left axes) and O 1s binding energy (right axes) as a result of the data analysis of the O 1s core level photoemission spectra (in Fig. 5). Vertical lines at exposure of 1 and 3 L indicate the exposure where the $c(2\times4)$ (0.5 ML) and $(2\times1)p2mg$ ordered structure are formed.

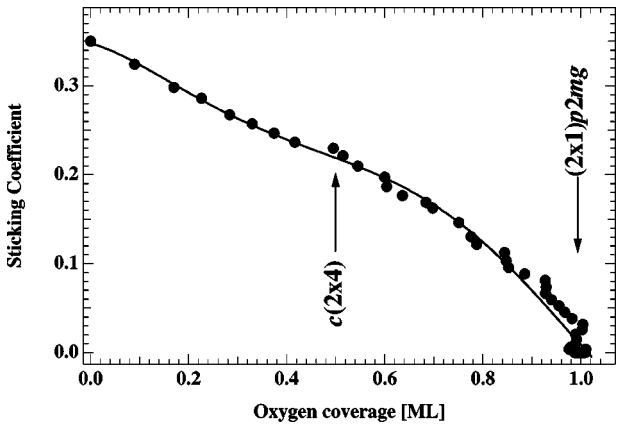

FIG. 7. Oxygen sticking coefficient: (filled markers) experimental data obtained from the O 1*s* core level measurements; (line) result of the fit with the Kisliuk model.

peak, initially located at 529.84 ± 0.01 eV, begins to shift towards lower binding energies to reach at saturation (4 L) a final value of 529.75 ± 0.01 eV. The experiment was repeated several times to confirm the existence of this small shift. The O 1*s* intensities (empty circles) obtained in the analysis were converted in absolute coverage (ML) by normalizing against the maximum O 1*s* intensity, achieved at saturation. As described in the previous paragraph the saturated surface is characterized by a sharp $(2\times1)p2mg$ structure at 1 ML which was used as a basis for the O coverage calibration. 1 ML is equal to the number of Ru surface atoms: 8.61×10^{14} atoms/cm^2 for the $(10\bar{1}0)$ plane. It is important to note the good agreement between XPS and SPALEED measurements. Both indicate that saturation is achieved at about 4L (compare Figs. 3 and 6).

The very weak shift in the O 1*s* binding energy, 75 ± 10 meV, is an indication that the O atoms are always located in the same adsorption site, in good agreement with the structural findings of Schwegmann *et al.*[3] The small energy shift could be ascribed to initial state effects (due to small differences in the adsorption geometry, i.e., O-Ru bond length) or to different electron screening of the core hole in the two cases.

The O 1*s* uptake data can also be used to calculate the oxygen sticking coefficient *s*, which is plotted, as first derivative of the uptake curve, in Fig. 7 as a function of the total coverage Θ. In our case the oxygen molecules require two adsorption sites to chemisorb dissociatively and as a consequence we can use the theoretical Kisliuk sticking probability curve for a two-adsorption site.[8] An initial sticking coefficient value s_0 of 0.35 ± 0.03 has been obtained.

The high energy resolution Ru $3d_{5/2}$ core level spectrum of the (1×1) clean surface is shown in Fig. 8, lower curve. In order to extract quantitative information from the core-level spectra, we analyzed the data by using, like for the O 1*s* peak, a Doniach-Sunjic function convoluted with a Gaussian. The best-fit parameter values were 0.27 ± 0.02 for the Lorentzian width, 0.095 ± 0.020 for the asimmetry parameter and 140 ± 20 meV for the Gaussian width. Three

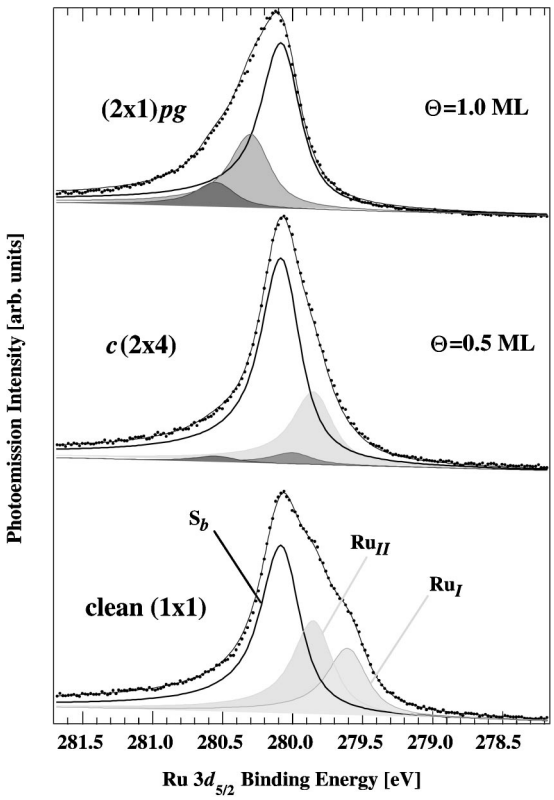

FIG. 8. Ru $3d_{5/2}$ core levels spectra from Ru$(10\bar{1}0)$ recorded at 300 K during oxygen uptake: (bottom) clean (1×1); (center) $c(2\times4)$; (top) $(2\times1)p2mg$. Fits of the surface components are presented.

components are present in the spectrum of the clean surface. We have recently found[9] that the peak at higher binding energy, S_b, is originated from the bulk atoms, while the other two, shifted by -480 ± 20 meV (Ru_I-yellow curve) and -240 ± 20 meV (Ru_{II}-light blue curve) respect to the bulk peak, correspond to first and second layer Ru atoms, respectively. The other spectra in Fig. 8 correspond to the $c(2\times4)$ (0.5 ML) and $(2\times1)p2mg$ (1.0 ML) oxygen structures. In fitting these spectra, we used the S_b, Ru_I, and Ru_{II} components, letting only their intensities as free parameters. The result of the procedure indicates that upon oxygen adsorption new components are needed in order to obtain a good fit of the experimental curves, as judged by χ-square analysis. As previously demonstrated[10] they correspond to different oxygen coordinated first- and second-layer Ru atoms. Intensities of the different components are plotted in Fig. 9 as a function of the oxygen coverage. They correspond to a series of Ru $3d_{5/2}$ spectra (not shown) measured during oxygen uptake. The fact that a complete series (about 30 curves) has been fitted using only the intensities of the different components as free parameters strongly reinforces the reliability of the whole procedure. At the beginning of the uptake the Ru_I component (yellow curve), linearly decreases in intensity and nearly disappears at 0.5 ML. This indicates that in the $c(2\times4)$ structure all first layer Ru atoms are

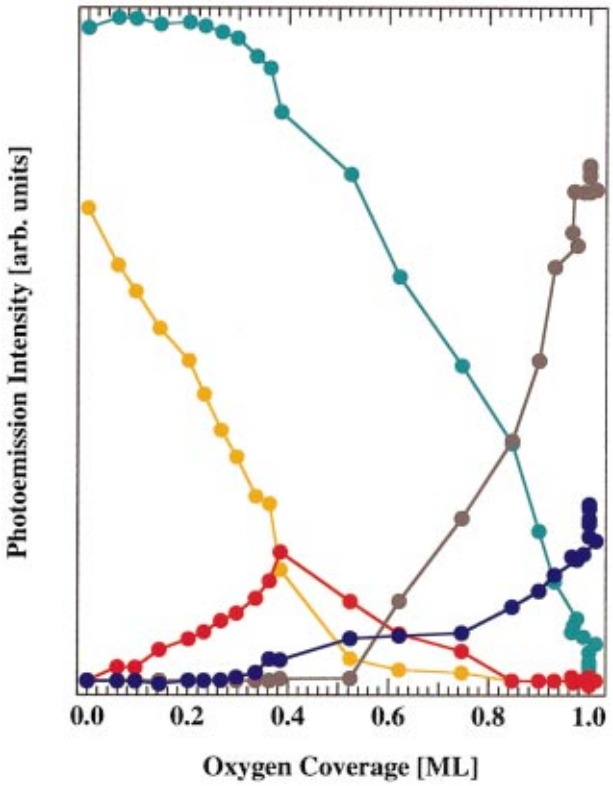

FIG. 9. (Color) Results of fit of the Ru3$d_{5/2}$ core levels spectra as a function of the oxygen coverage. Colored curves are: (yellow) first layer Ru, (light blue) second layer Ru, (red) first layer single oxygen bonded Ru, (blue) second layer two oxygen bonded Ru and (gray) first layer two oxygen bonded Ru.

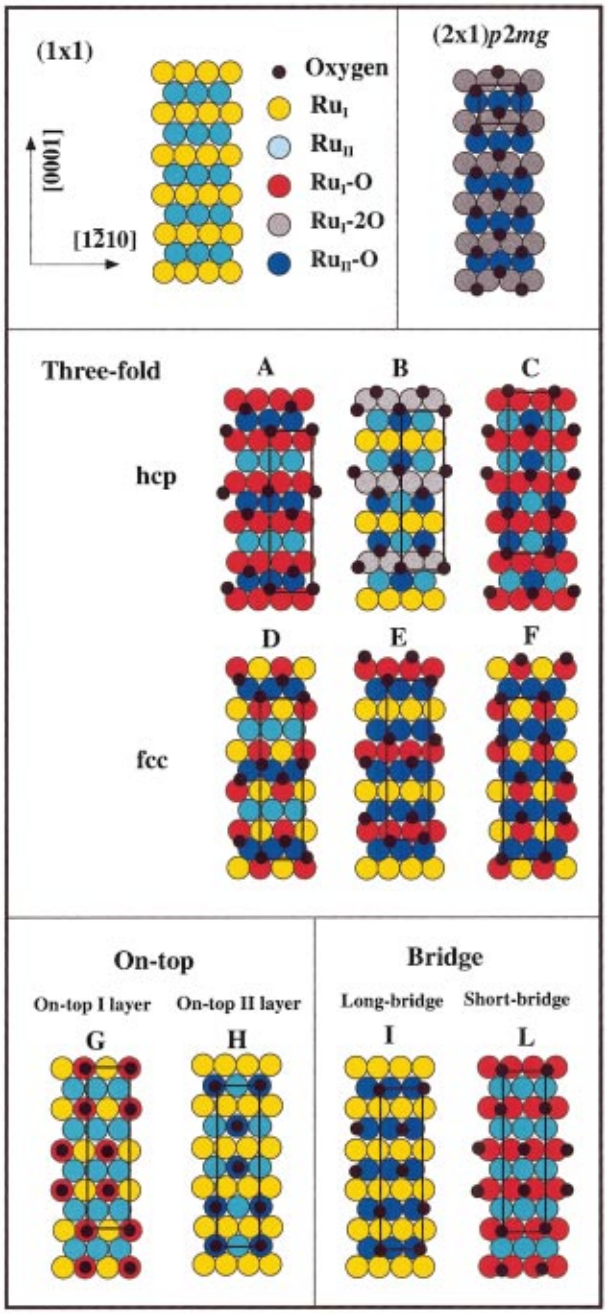

FIG. 10. (Color) Possible models for the Ru(10$\bar{1}$0)-$c(2\times4)$-2O structure, with oxygen sitting in three-fold hcp, three-fold fcc, on-top, short-bridge and long-bridge sites. The upper panel presents (1×1) and $(2\times1)p2mg$ models. Colors correspond to: (yellow) first layer Ru, (light blue) second layer Ru, (red) first layer single oxygen bonded Ru, (blue) second layer two oxygen bonded Ru and (gray) first layer two oxygen bonded Ru.

bonded with oxygen. In the same range of coverage the Ru_{II} peak (light blue peak) decreases but does not disappear. At low coverage (<0.5 ML) other two peaks appear at -85 ± 20 meV (red peak) and $+465\pm20$ meV (blue peak) respect to the bulk peak. Their behavior for $\Theta>0.5$ ML is very different: the first one decreases in intensity and disappears at saturation, while the second one increases up to saturation. Another component (gray curve), positioned at $+215\pm20$ meV with respect to the bulk peak, grows linearly above 0.5 ML and reaches its maximum at 1 ML, just when the best $(2\times1)p2mg$ structure is formed. In a previous report we have already assigned the different components appearing during the uptake process, as originated by Ru atoms multiply coordinated with oxygen.[10] This approach has been already used by Riffe and Wertheim[11] and by Ynzunza[12] for the O/W(110) system and by Andersen *et al.* for CO on Pd(110).[13]

In Fig. 10 we illustrate all the possible $c(2\times4)$ structures formed by oxygen adsorption at 0.5 ML with different adsorption site and geometrical arrangement. On the basis of our results, we can exclude those with first layer unperturbed Ru_I atoms (yellows atoms). Models with oxygen in threefold fcc site (*D*, *E*, and *F*) and on-top site (*G* and *H*), and also models *B* and *I*, are not compatible with our observation. Also model *L* can be excluded because at 0.5 ML the second layer clean component Ru_{II} should be not changed in intensity contrary to what is experimentally observed. Our conclusion is therefore that oxygen sits in threefold hcp sites, in agreement with previous structural investigations.[3] The differences with respect to the expected linear decrease in intensity with coverage can be due to photoelectron diffraction effects that could strongly alter photoemission intensity, as

demonstrated for many systems.[14] We interpret therefore the peak at $-85\pm$ meV as originated from the first-layer Ru atoms single bonded with oxygen (Ru_I-O), while the other component at $+465$ meV as due to single oxygen bonded with Ru second layer atoms (Ru_{II}-O). Also the trends for $\Theta > 0.5$ ML are in accord with this interpretation. In fact, with increasing the oxygen coverage, the Ru_I-O component decreases and disappears at saturation. Above 0.5 ML also the $(2\times1)p2mg$ structure begins to grow. The formation is related to the gray component originated by first layer double-bonded Ru atoms (Ru_I-2O); simultaneously the single-bonded second-layer Ru atoms (Ru_{II}-O) reach the maximum value at 1 ML.

IV. DISCUSSION

As for all overlayer structures, the formation of a certain configuration with long-range order is caused by the existence of interactions between the adsorbed atoms. Below 0.3–0.4 L, i.e., over the whole coverage range $0<\Theta<0.25$ ML, in both the experimentally measured $I_{1/2,3/4}$ and $I_{0,1/2}$, the fractional-order spots are so weak that both the beam sharpness and the intensity curve are difficult to evaluate and therefore have not been reported in Figs. 1 and 2. This implies that the tendency for island formation is not very strong, in agreement with the extrapolated non-linear increase of the intensity shown in Fig. 1 (dotted curve). This means that the interaction energies at long distances are lower than the thermal energy K_BT, 25 meV in our case. At low coverage the oxygen atoms are almost randomly distributed over the surface in a lattice gas configuration. However, as the coverage increases, the linear increase of the diffraction spots (shown in Figs. 1 and 2) indicates an island growth process: the threefold hcp bonded oxygen atoms exhibit a tendency to two-dimensional ordering above ≈ 0.7 L, resulting in the formation of the $c(2\times4)$ structure at 1.0 L. The FWHM of both (1/2,3/4) and (0,1/2) diffraction spots indicate that the ordering process proceeds more easily along the $[1\bar{2}10]$ direction than on the [0001], as a results of the surface anisotropy: oxygen starts to form zig-zag chains along the $[1\bar{2}10]$ direction, but the chains are not well ordered in the [0001] direction. Structures of this type where reported for oxygen adsorption on the Rh(110) (Ref. 15) and Pd(110) (Ref. 16) surfaces and on Co $[10\bar{1}0]$.[17] The residual disorder, prior the $c(2\times4)$ formation, is determined by the existence of small islands, with oxygen sitting in one of the two equivalent sublattices (*A*/zig-zag and *B*/zag-zig). The zig-zag rows formation with a *ANBNANB* (*N* means row not occupied) is not established in the long-range and the most probable configuration is with adjacent empty rows, i.e., for example *ANBNNBNA*. These results correlate with the SCLS data: the Ru_{II} component (hell blue curve in Fig. 9) is not equal to zero, thus indicating the presence in the $c(2\times4)$ of clean second layer atoms not bonded with oxygen. However SCLS data are not sufficient to discern between A and C $c(2\times4)$ structural models. The attractive interactions between the oxygen atoms within the row (i.e., along the $[1\bar{2}10]$ direction) is very strong and results in the formation of zig-zag chains when the $c(2\times4)$ structure is completely formed. We want to point out that the interaction between adjacent zig-zag rows is very important even at moderate low coverage: the rows should be out-of-phase in order to form a $c(2\times4)$ structure (*ANBNANB* configuration), instead of a $(2\times2)p2mg$ structure (*ANAN* or *BNBN* configuration) at the same coverage. For this reason we conclude that the next-nearest neighbor oxygen rows interaction is quite strong. In the coverage range $0.3<\Theta<0.65$ ML a movement of the (1/2,3/4) diffraction spots is observed (Fig. 4) which obviously reflects a transformation of the overlayer arrangement. Beam shifts of this type have been already observed and can be considered as the result of a dynamical arrangement of parallel [0001] rows with a distribution of the spacings from $3a$ to a in the $[1\bar{2}10]$ direction (a is the lattice spacing along $[12\bar{1}0]$). Only at the intermediate coverage $0.45<\Theta<0.55$ the spot position is nearly constant, thus indicating that this is the range of existence of the $c(2\times4)$ structure. At 0.5 ML the $c(2\times4)$ structure present island with an average size of 130 Å$\times$280 Å.

The slope of the (1/2,3/4) diffraction spots movement above 0.58 ML indicates that the disruption of the $c(2\times4)$ island is faster than the formation. The reason of this can be related to the short-range oxygen interactions at coverage larger than 0.5 ML: when a molecule arrives on the $c(2\times4)$ surface and dissociates, the antiphase rows local configuration is forbidden by the strong repulsion between oxygen atoms sitting in adjacent three-fold hcp sites along the [0001] direction.

The sticking coefficient behavior against the oxygen coverage is a further important indicator of the adsorption mechanism. Our curve presents a linear decrease until the formation of the $c(2\times4)$ structure, indicating a mechanism in which trapping can take place into a molecular precursor state, with subsequent diffusion to a threefold site when the dissociation can take place. At low coverage the three-fold oxygen adsorbs with a disordered configuration up to the formation of the $c(2\times4)$ related diffraction spots at ≈ 0.34 ML. As the adsorption proceeds the reduced number of available free site pairs will immediately affect the adsorption rate. Only at coverage higher than 0.5 ML, in correspondence of the formation of the Ru_I-2O species, the repulsive O-O interactions reduce the probability of finding appropriate three-fold hcp site pairs for dissociation of the molecular precursor. In fact the $c(2\times4)$ structure proposed by Schwegmann *et al.* does not offers two nearby empty sites. This implies that the O atoms must move around the surface to create new adsorption sites: it is the ordering of the adlayer that exerts its influence on the adsorption probability and just above 0.5 ML the sticking coefficient decreases faster.

V. CONCLUSIONS

By combining a long-range order technique like spot profile analysis LEED and a local probe like XPS we have studied the formation of the $c(2\times4)$ and $(2\times1)p2mg$ structures on Ru$(10\bar{1}0)$. The low coverage structure is characterized by a single Ru first layer species (Ru single

bonded with oxygen) while at saturation oxygen sits in the same adsorption site (three-fold hcp) forming two bonds with Ru first layer atoms. A qualitative description of the mechanism of the overlayer formation in terms of adsorbate-adsorbate interaction has been proposed for the whole coverage range.

ACKNOWLEDGMENTS

The authors gratefully acknowledge stimulating discussions with Maya Kiskinova. Financial support from the Italian MURST under the program COFIN99 is acknowledged.

*Corresponding author. Email address: baraldi@elettra.trieste.it FAX: +39-0403758565.

[1] T.W. Orent and R.S. Hansen, Surf. Sci. **67**, 325 (1977).
[2] S. Poluston, M. Tikhov, and R. Lambert, Surf. Rev. Lett. **1**, 655 (1994).
[3] S. Schwegmann, A.P. Seistonen, V. De Renzi, H. Dietrich, H. Bludau, M. Gierer, H. Over, K. Jacobi, M. Scheffler, and G. Ertl, Phys. Rev. B **57**, 487 (1998).
[4] A. Baraldi, M. Barnaba, B. Brena, D. Cocco, G. Comelli, S. Lizzit, G. Paolucci, and R. Rosei, J. Electron Spectrosc. Relat. Phenom. **76**, 145 (1995).
[5] A.E. Ferdinand and M.E. Fisher, Phys. Rev. **185**, 832 (1969).
[6] D.P. Landau, Phys. Rev. B **13**, 2997 (1976).
[7] N. Mårtensson and A. Nilsson, in *Application of Synchrotron Radiation* (Springer, New York).
[8] P. Kisliuk, J. Phys. Chem. Solids **3**, 95 (1957); **5**, 78 (1958).
[9] A. Baraldi, S. Lizzit, G. Comelli, A. Goldoni, Ph. Hofmann, and G. Paolucci, Phys. Rev. B **61**, 4534 (2000).
[10] A. Baraldi, S. Lizzit, and G. Paolucci, Surf. Sci. **457**, L354 (2000).
[11] D.M. Riffe and G.K. Wertheim, Surf. Sci. **399**, 248 (1998).
[12] R. X. Ynzunza, Ph.D. thesis, University of California, Berkeley, 1998 (unpublished).
[13] J.N. Andersen, M. Qvarford, R. Nyholm, S.L. Sorensen, and C. Wigren, Phys. Rev. Lett. **67**, 2822 (1991).
[14] D.P. Woodruff and A.M. Bradshaw, Rep. Prog. Phys. **57**, 1029 (1994).
[15] G. Comelli, V.R. Dhanak, M. Kiskinova, K.C. Prince, and R. Rosei, Surf. Sci. Rep. **32**, 165 (1998).
[16] H. Tanaka, J. Yoshinobu, and M. Kawai, Surf. Sci. **327**, L505 (1997).
[17] M. Gierer, H. Over, P. Pech, E. Schwarz, and K. Christmann, Surf. Sci. **370**, L201 (1997).